

---

# Conditional Diffusion Models for Uncertainty Estimation in Super Resolution Microscopy

---

Anonymous Author(s)

Affiliation

Address

email

## Abstract

1 The field of deep generative modeling for image translation has experienced a  
2 boom in research in the past few years, with various tools developed to estimate  
3 different types of uncertainty. Yet, many powerful models in image translation are  
4 selected and trained based upon reconstruction loss and therefore are unable report  
5 uncertainty in their outputs. Uncertainty quantification is a necessary modeling  
6 component in many high-risk applications and in the sciences. In order to quantify  
7 uncertainty in otherwise deterministic models, we propose a hybrid generative  
8 modeling framework based denoising diffusion probabilistic models (DDPMs).  
9 Specifically, our model learns a distribution on the true image latent in the input  
10 conditioned on the network output, in order to represent the posterior on recon-  
11 structions. We apply this framework to the task of single molecule localization in  
12 fluorescence microscopy, and demonstrate that blending the DeepSTORM archi-  
13 tecture with a DDPM permits uncertainty quantification of kernel density estimates  
14 (KDEs) regressed by DeepSTORM. Our results suggest the proposed solution is an  
15 interesting addition to the modeling toolkit for fluorescence microscopists and the  
16 field of deep image translation in general.

## 1 Introduction

18 Deep learning has attracted tremendous attention from researchers in the natural sciences, with  
19 several foundational applications arising in microscopy, e.g., (Weigert 2018; Falk 2019). Recently,  
20 the application of deep image translation in single-molecule localization microscopy (SMLM) has  
21 received considerable interest (Ouyang 2018; Nehme 2020; Speiser 2021). SMLM techniques are  
22 a mainstay of fluorescence microscopy and can be used to produce a pointillist representation of  
23 living cells at diffraction-unlimited precision (Rust 2006; Betzig 2006). As this technology enables  
24 increasingly precise measurements of the cellular environment, there is an increasing need for  
25 machine learning methods to report uncertainty for quality control.

26 In previous applications of deep models to localization microscopy, super-resolution images can be  
27 recovered from a sparse set of localizations with conditional generative adversarial networks (Ouyang  
28 2018) or kernel density estimation can be performed using convolutional networks (Nehme 2020;  
29 Speiser 2021). Here, we focus on the latter class of models which perform single molecule localization  
30 using neural networks. In this approach, one estimates molecular coordinates by predicting kernel  
31 density estimates (KDEs)  $y$ , which are latent in the raw data  $x$ , using a convolutional neural network.  
32 Importantly, inferences in SMLM are often necessarily made on a single measurement, thus common  
33 measures of model performance are based on localization errors computed over ensembles of  
34 simulated images. However, this choice precludes computation of aleatoric uncertainty at test time  
35 under a fixed model, and may result in the application of models to out of distribution datasets.

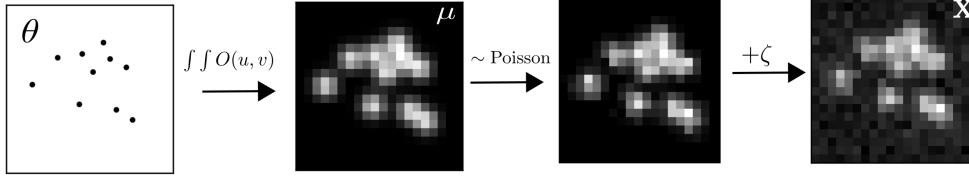


Figure 1: Generative model of single molecule localization microscopy images

Bayesian probability theory offers us mathematically grounded tools to reason about model uncertainty, but these usually come with a prohibitive computational cost. A few approaches to avoiding this intractability have been deterministic uncertainty quantification (Amersfoort 2020), ensembling (Lakshminarayanan et al., 2017) or Monte Carlo dropout (Gal and Ghahramani, 2016). Here, we report a method which models estimates uncertainty in KDE predictions by learning a distribution on the true image latent in the input conditioned on the network output, in order to represent the posterior on reconstructions. Our approach preserves image structure and produces pixel-wise uncertainties, which can be used for out of distribution sample detection or filtering. We choose to model this distribution using a denoising diffusion probabilistic models (DDPM), referred to here as simply “diffusion model”. Such models are well suited conditional image generation tasks, demonstrating promising results in detail reconstruction, while directly providing uncertainties in model predictions (Saharia 2021). Our approach could be readily integrated with existing localization performance measures to address both model accuracy on training data and precision on datasets produced by experiments.

## 2 Background

### 2.1 Image Likelihood and Localization Error

The central objective of single molecule localization microscopy is to infer a set of molecular coordinates  $\theta$  from measured low resolution images  $\mathbf{x}$ . The likelihood on measured low-resolution images  $p(\mathbf{x}|\theta)$  is taken to be a convolution of Gaussian and Poisson PDFs, due to shot noise and sensor readout noise

$$p(\mathbf{x}_k|\theta) = A \sum_{q=0}^{\infty} \frac{1}{q!} e^{-\omega_k} \omega_k^q \frac{1}{\sqrt{2\pi}\sigma_k} e^{-\frac{(\mathbf{x}_k - g_k q - o_k)^2}{2\sigma_k^2}} \quad (1)$$

where  $p(\zeta_k) = \mathcal{N}(o_k, \sigma_k^2)$  and  $p(s_k) = \text{Poisson}(\omega_k)$ ,  $A$  is some normalization constant. In practice, (4) is difficult to work with, so we look for an approximation. We will use a Poisson-Normal approximation for simplification, valid under a range of experimental conditions (Huang 2013)

$$\mathbf{x}_k \sim \text{Poisson}(\omega'_k) \quad (2)$$

where  $\omega'_k = \omega_k + \sigma_k^2$ . This result can be seen from the fact the the convolution of two Poisson distributions is also Poisson.

Reliable estimation of  $\theta$  from  $\mathbf{x}$  requires performance metrics for model selection. We use the Fisher information as an information theoretic criteria to assess the model quality, with respect to the root mean squared error (RMSE) of our predictions of  $\theta$  (Chao 2016). The Poisson log-likelihood  $\ell(\mathbf{x}|\theta)$  is also convenient for computing the Fisher information matrix (Smith 2010) and thus the Cramer-Rao lower bound, which bounds the variance of a statistical estimator of  $\theta$ , from below i.e.,  $\text{var}(\hat{\theta}) \geq I^{-1}(\theta)$ . The Fisher information is straightforward to compute under the Poisson log-likelihood, which is detailed in the Appendix

$$\mathcal{I}_{ij}(\theta) = \mathbb{E}_{\theta} \left( \frac{\partial \ell}{\partial \theta_i} \frac{\partial \ell}{\partial \theta_j} \right) = \sum_k \frac{1}{\omega'_k} \frac{\partial \omega'_k}{\partial \theta_i} \frac{\partial \omega'_k}{\partial \theta_j} \quad (3)$$

## 68 2.2 Kernel density estimation with deep networks

69 Direct optimization of the log-likelihood in (7) from observations  $\mathbf{x}$  alone is challenging when  
70 fluorescent emitters are dense within the field of view and fluorescent signals significantly overlap.  
71 Convolutional neural networks (CNN) have recently been used in fluorescence microscopy to extract  
72 parameters describing fluorescent emitters such as color, emitter orientation,  $z$ -coordinate, and  
73 background signal (Zhang 2018; Kim 2019; Zelger 2018). For localization tasks, CNNs typically  
74 employ upsampling layers to reconstruct Bernoulli probabilities of emitter occupancy (Speiser 2021)  
75 or kernel density estimates with higher resolution than experimental measurements (Nehme 2020).  
76 Kernel density estimates are the most common data structure used in SMLM, and can be easily  
77 generated from molecular coordinates using well-understood models of the optical impulse response  
78 (Zhang 2007). In addition, models of the optical impulse response can be combined with Poisson  
79 likelihood (2) to generate ground-truth data for model training, which is often not available in  
80 experimental contexts.

81 The DeepSTORM CNN, initially proposed in (Nehme 2020) for 3D localization, can be viewed  
82 as a deep kernel density estimator, reconstructing kernel density estimates  $\mathbf{y}$  from low-resolution  
83 inputs  $\mathbf{x}$ . We utilize a simplified form of the original architecture for 2D localization, which we  
84 denote  $\phi$  hereafter, which consists of three main modules: a multi-scale context aggregation module,  
85 an upsampling module, and a prediction module. For context aggregation, the architecture utilizes  
86 dilated convolutions to increase the receptive field of each layer. The upsampling module is then  
87 composed of two consecutive 2x resize-convolutions, computed by nearest-neighbor interpolation,  
88 to increase the lateral resolution by a factor of 4. For a common sCMOS camera, each pixel has a  
89 lateral size of approximately 108 nanometers, giving approximately 27 nanometer pixels in the KDE.  
90 The terminal prediction module contains three additional convolutional blocks for refinement of the  
91 upsampled image, followed by an element-wise HardTanh.

## 92 3 Diffusion Model for SMLM

93 We consider datasets  $(\mathbf{x}_i, \mathbf{y}_i, \hat{\mathbf{y}}_i)_{i=1}^N$  of observed images  $\mathbf{x}_i$  true kernel density estimate (KDE) images  
94  $\mathbf{y}_i$ , and KDE estimates  $\hat{\mathbf{y}}_i = \phi(\mathbf{x}_i)$ . Observations  $\mathbf{x}_i$  are generated under the image degradation  
95 model. We aim to develop a framework for sampling from  $p(\hat{\mathbf{y}}|\mathbf{x}, \mathbf{y})$ .

## 96 4 Conditional Diffusion Model

97 Point estimates  $\hat{\mathbf{y}}_i$  produced by the DeepSTORM architecture lack uncertainty quantification. To  
98 address this, we propose a DDPM to model the conditional distribution  $p(\hat{\mathbf{y}}|\mathbf{x}, \mathbf{y})$ . Consider the fac-  
99 torization  $p(\hat{\mathbf{y}}|\mathbf{x}, \mathbf{y})p(\mathbf{x}|\mathbf{y})p(\mathbf{y}) = p(\mathbf{x}|\mathbf{y}, \hat{\mathbf{y}})p(\mathbf{y}|\hat{\mathbf{y}})p(\hat{\mathbf{y}})$ . Given that  $\mathbf{x}$  is conditionally independent  
100 of  $\hat{\mathbf{y}}$ , we find

$$p_{\Psi}(\hat{\mathbf{y}}|\mathbf{x}, \mathbf{y}) = p(\mathbf{y}|\hat{\mathbf{y}})$$

101 Evidently, the DDPM  $\Psi$  can be trained on pairs  $(\mathbf{y}_i, \hat{\mathbf{y}}_i)_{i=1}^N$ . The conditional DDPM generates a  
102 target KDE  $\mathbf{y}_0$  in  $T$  refinement steps. Starting with a pure noise image  $\mathbf{y}_T \sim \mathcal{N}(0, \mathbf{I})$ , the model  
103 iteratively refines the KDE through successive iterations according to learned conditional transition  
104 distributions  $p(\mathbf{y}_{t-1}|\mathbf{y}_t, \cdot)$  such that  $\mathbf{y}_0 \sim p(\mathbf{y}|\hat{\mathbf{y}})$

### 105 4.1 Gaussian Diffusion

106 Diffusion models (Sohl-Dickstein 2015; Ho 2020) are a class of generative models inspired by  
107 nonequilibrium statistical physics, which slowly destroy structure in a data distribution  $p(\mathbf{y}_0|\mathbf{x})$  via a  
108 fixed Markov chain referred to as the *forward process*. In the present context, the forward process  
109 gradually adds Gaussian noise to the KDE  $\mathbf{y}$  according to a variance schedule  $\beta_{0:T}$

$$q(\mathbf{y}_t|\mathbf{y}_0) = \prod_{t=1}^T q(\mathbf{y}_t|\mathbf{y}_{t-1}) \quad q(\mathbf{y}_t|\mathbf{y}_{t-1}) = \mathcal{N}\left(\sqrt{1-\beta_t}\mathbf{y}_{t-1}, \beta_t \mathbf{I}\right) \quad (4)$$

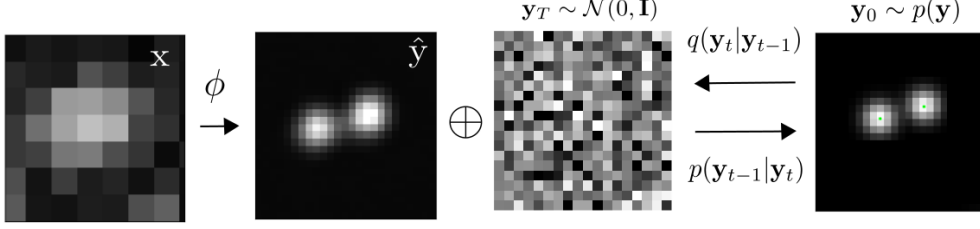


Figure 2: Conditional diffusion model for sampling kernel density estimates

110 An important property of the forward process is that it admits sampling  $\mathbf{y}_t$  at an arbitrary timestep  $t$   
 111 in closed form (Ho 2020). Using the notation  $\alpha_t := 1 - \beta_t$  and  $\gamma_t := \prod_{s=1}^t \alpha_s$ , we have

$$q(\mathbf{y}_t|\mathbf{y}_0) = \mathcal{N}(\sqrt{\gamma_t}\mathbf{y}_0, (1 - \gamma_t)\mathbf{I}) \quad (5)$$

112 The usual procedure is then to learn a parametric representation of the *reverse process*, and therefore  
 113 generate samples from  $p(\mathbf{y}_0)$ , starting from noise. Formally,  $p_\theta(\mathbf{y}_0|\hat{\mathbf{y}}) = \int p_\theta(\mathbf{y}_{0:T}|\hat{\mathbf{y}})d\hat{\mathbf{y}}_{1:T}$  where  
 114  $\mathbf{y}_t$  is a latent representation with the same dimensionality of the data.  $p_\theta(\mathbf{y}_{0:T}|\hat{\mathbf{y}})$  is a Markov process,  
 115 starting from a noise sample  $p_\theta(\mathbf{y}_T) = \mathcal{N}(0, \mathbf{I})$ .

$$p_\theta(\mathbf{y}_{0:T}) = p_\theta(\mathbf{y}_T) \prod_{t=1}^T p_\theta(\mathbf{y}_{t-1}|\mathbf{y}_t) \quad p_\theta(\mathbf{y}_{t-1}|\mathbf{y}_t) = \mathcal{N}(\mu_\theta(\mathbf{y}_t), \beta_t\mathbf{I}) \quad (6)$$

116 where we reuse the variance schedule of the forward process (Ho 2020). We seek to learn a denoising  
 117 model  $\mu_\theta$  which computes the mean of the Gaussian transition density at each time step  $t$ . For all  
 118  $t > 0$ , the mean of the transition density is computed as

$$\mu_\theta(\mathbf{y}_t, \hat{\mathbf{y}}, \gamma_t) = \frac{1}{\sqrt{\alpha_t}} \left( \mathbf{y}_t - \frac{(1 - \alpha_t)}{\sqrt{1 - \gamma_t}} f_\theta(\mathbf{y}, \hat{\mathbf{y}}, \gamma_t) \right) \quad (7)$$

119 where  $f_\theta$  is a neural network. Only at  $t = 0$  is this mean directly a function of  $\mathbf{x}$ .

## 120 4.2 Optimization of the Denoising Model

121 To reverse the diffusion process, we optimize a neural denoising model  $f_\theta$  that takes as input  $\hat{\mathbf{y}}$  and a  
 122 noisy target image  $\mathbf{y}_t \sim q(\mathbf{y}_t|\mathbf{y}_0)$ . That is, this noisy target image  $\mathbf{y}_t$  is drawn from the marginal  
 123 distribution of noisy images at a time step  $t$  of the forward diffusion process.

$$\mathbf{y}_t = \sqrt{\gamma_t}\mathbf{y}_0 + \sqrt{1 - \gamma_t}\epsilon, \quad \epsilon \sim \mathcal{N}(0, \mathbf{I}) \quad (8)$$

124 In addition to a source image  $\mathbf{y}_0$  and a noisy target image  $\mathbf{y}_t$ , the denoising model  $f_\theta$  takes as input  
 125 the sufficient statistics for the variance of the noise  $\gamma$ , and is trained to predict the noise vector  $\epsilon$ .  
 126 We make the denoising model aware of the level of noise through conditioning on a scalar  $\gamma$ . The  
 127 proposed objective function for training  $f_\theta$  is

$$\mathbb{E}_{(\hat{\mathbf{y}}, \mathbf{y}_0)(\epsilon, \gamma)} \left[ f_\theta \left( x, \sqrt{\gamma_t}\mathbf{y}_0 + \sqrt{1 - \gamma_t}\epsilon \mid \mathbf{y}_t, \gamma \right) - \epsilon \right], \quad (9)$$

128 where  $(\hat{\mathbf{y}}, \mathbf{y}_0)$  is sampled from the training dataset and  $\gamma \sim p(\gamma)$ . The distribution of  $\gamma$  has a big  
 129 impact on the quality of the model and the generated outputs. For our training noise schedule, we  
 130 use a piecewise distribution for  $\gamma$ ,  $p(\gamma) = \frac{1}{T} \sum_{t=1}^T U(\gamma_{t-1}, \gamma_t)$  (Nanxin 2021). Specifically, during  
 131 training, we first uniformly sample a time step  $t \sim \{0, \dots, T\}$  followed by sampling  $\gamma \sim U(\gamma_{t-1}, \gamma_t)$ .  
 132 We set  $T = 100$  in all our experiments.

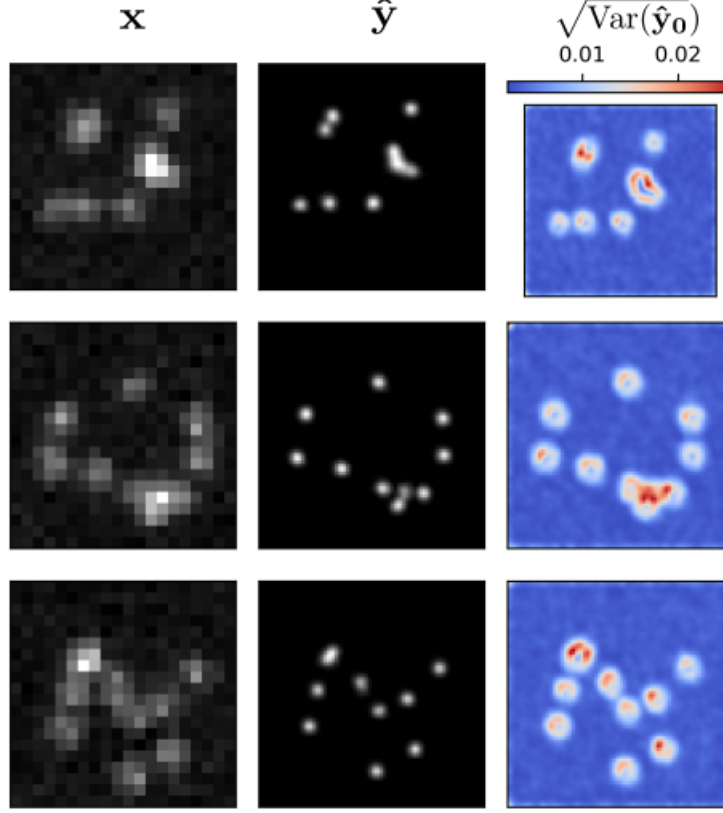


Figure 3: Kernel density estimates for various signal to noise ratios (SNR)

### 4.3 Optimization of the DeepSTORM architecture

A first pass at localization treats localization as a binary classification problem, such that 0 denotes a vacant pixel and 1 denotes an occupied pixel containing an emitter. Direct learning of pixel-wise classification with cross-entropy loss leads to an imbalance of occupied and unoccupied pixels in dense localization problems (Nehme 2020). CE loss is usually either weighted [51], replaced with a Focal loss [52], or applied to a "blobbed" version of the desired boolean volume e.g. by placing a disk around each GT position [53–55]. Alternative methods take a soft version of the binary classification problem. That is, by placing a small Gaussian around each GT position (e.g. with std of 1 pixel), and matching continuous heatmaps, backpropagation yields more meaningful gradients and eases the learning process convergence.

Localization heatmaps thus form a natural encoding for SMLM images, which can be input to our conditional diffusion model. Therefore, to encode raw data  $\mathbf{x}$  into a more tractable representation, we train the DeepSTORM architecture (Nehme 2020). Raw coordinates  $\theta$  are binned into an upsampled image  $\mathbf{z}$ .

$$\mathcal{L}(\mathbf{y}, \hat{\mathbf{y}}) = \|\mathbf{y} - \hat{\mathbf{y}}\|^2$$

## 5 Experiments

Training data was simulated under the image degradation model, drawing coordinates uniformly over a disc. We set  $T = 100$  for all experiments and treat forward process variances  $\beta_t$  as hyperparameters, with a linear schedule from  $\beta_0 = 10^{-4}$  to  $\beta_T = 10^{-2}$ . These constants were chosen to be small relative to data scaled to  $[-1, 1]$ , ensuring that reverse and forward processes have approximately the same functional form while keeping the signal-to-noise ratio at  $x_T$  as small as possible ( $L_T = D_{KL}(q(x_T|x_0)||\mathcal{N}(0, I)) \approx 10^{-5}$  bits per dimension in our experiments).

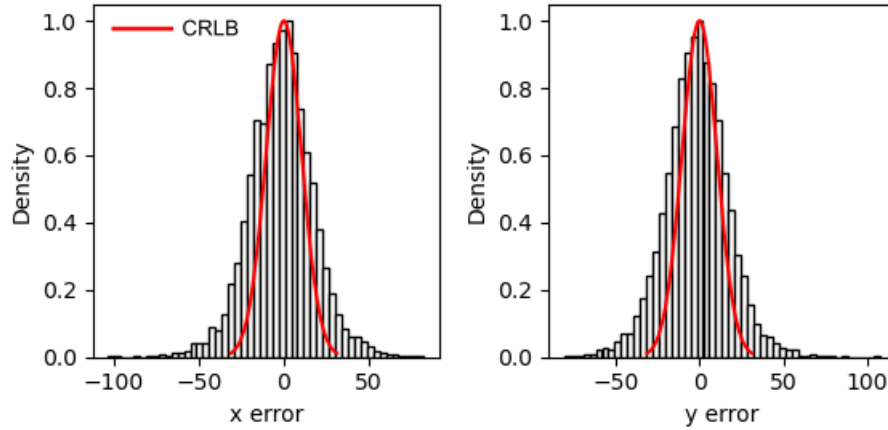


Figure 4: Localization errors of the trained model

To represent the reverse process, we used the DDPM architecture based on a U-Net backbone (Ho 2020). Parameters are shared across time, which is specified to the network using the Transformer sinusoidal position embedding  $\gamma$ . We use self-attention at the  $16 \times 16$  feature map resolution  $\gamma$ . Details are in Appendix A.

and the channel multipliers at different resolutions (see Appendix A for details). To condition the model on the input  $x$ , we up-sample the low-resolution image to the target resolution using bicubic interpolation. The result is concatenated with  $y_t$  along the channel dimension. We experimented with more sophisticated methods of conditioning, such as using  $\gamma$ , but we found that the simple concatenation yielded similar generation quality.

## 6 Related Work

### 6.1 Diffusion Models

Prior work of diffusion models  $\gamma$  require 1-2k diffusion steps during inference, making generation slow for large target resolution tasks. We adapt techniques from  $\gamma$  to enable more efficient inference. Our model conditions on  $\gamma$  directly (vs  $t$  as in  $\gamma$ ), which allows us flexibility in choosing the number of diffusion steps, and the noise schedule during inference. This has been demonstrated to work well for speech synthesis  $\gamma$ , but has not been explored for images. For efficient inference, we set the maximum inference budget to 100 diffusion steps, and hyper-parameter search over the inference noise schedule. This search is inexpensive as we only need to train the model once  $\gamma$ . We use FID on held-out data to choose the best noise schedule, as we found PSNR did not correlate well with image quality.

## 7 Conclusion

## References

- [1] Nehme, E., et al. *DeepSTORM3D: dense 3D localization microscopy and PSF design by deep learning*. Nature Methods 17, 734–740 (2020).
- [2] Ouyang, W., et al. *Deep learning massively accelerates super-resolution localization microscopy*. Nature Biotechnology 36, 460–468 (2018).
- [3] Speiser, A., et al. *Deep learning enables fast and dense single-molecule localization with high accuracy*. Nature Methods 18, 1082–1090 (2021).
- [4] Sohl-Dickstein J., et al. *Deep unsupervised learning using nonequilibrium thermodynamics*. ICLR (2015).

- [5] Ho J., et al. *Denoising Diffusion Probabilistic Models*. Advances in Neural Information Processing Systems (2015).
- [6] Nanxin C., et al. *WaveGrad: Estimating Gradients for Waveform Generation*. ICLR (2021).
- [4] Chao, J., et al. *Fisher information theory for parameter estimation in single molecule microscopy: tutorial*. Journal of the Optical Society of America A 33, B36 (2016).
- [5] Schermelleh, L. et al. *Super-resolution microscopy demystified*. Nature Cell Biology vol. 21 72–84 (2019).
- [6] Zhang, B., et al. *Gaussian approximations of fluorescence microscope point-spread function models*. (2007).
- [7] Smith, C.S., *Fast, single-molecule localization that achieves theoretically minimum uncertainty*. Nature Methods 7, 373–375 (2010).
- [8] Nieuwenhuizen, R., et al. *Measuring image resolution in optical nanoscopy*. Nature Methods 10, 557–562 (2013).
- [9] Huang, F., et al. *Video-rate nanoscopy using sCMOS camera-specific single-molecule localization algorithms*. Nat Methods 10, 653–658 (2013).
- [10] Rust, M., et al. *Sub-diffraction-limit imaging by stochastic optical reconstruction microscopy (STORM)*. Nat Methods 3, 793–796 (2006).
- [11] Betzig, E., et al. *Imaging intracellular fluorescent proteins at nanometer resolution*. Science 313, 1642–1645 (2006).
- [12] Weigert, M., et al. *Content-aware image restoration: pushing the limits of fluorescence microscopy*. Nat. Methods 15, 1090 (2018).
- [13] Falk, T., et al. *U-net: deep learning for cell counting, detection, and morphometry*. Nat. Methods 16, 67–70 (2019).
- [14] Boyd, N., et al. *DeepLoco: fast 3D localization microscopy using neural networks*. Preprint at bioRxiv <https://doi.org/10.1101/267096> (2018)
- [15] Zelger, P., et al. *Three-dimensional localization microscopy using deep learning*. Opt. Express 26, 33166–33179 (2018)
- [16] Zhang, P., et al. *Analyzing complex single-molecule emission patterns with deep learning*. Nat. Methods 15, 913 (2018)
- [17] Saharia, C., et al. *Image Super-Resolution via Iterative Refinement*. Preprint at arXiv <https://doi.org/10.48550/arXiv.2104.07636> (2021)
- [18] Kim, T., et al. *Information-rich localization microscopy through machine learning*. Nat Commun 10, 1996 (2019).

## A Appendix

Standard SMLM localization algorithms based on maximum likelihood estimators or least squares optimization require tight control of activation and reactivation to maintain sparse emitters, presenting a tradeoff between imaging speed and labeling density. Recently, deep models have generalized SMLM to densely labeled structures by predicting high-resolution kernel density estimates (KDEs) from low resolution images with convolutional networks. However, estimated KDEs may contain irregularities due to finite sample sizes and limited model capacity.

Single molecule localization microscopy (SMLM) relies on the temporal resolution of fluorophores whose spatially overlapping point spread functions would otherwise render them unresolvable at the detector. Common strategies for the temporal separation of molecules involve molecular photoswitching from dark to fluorescent states, permitting resolution of fluorophores beyond the diffraction limit. Estimation of molecular coordinates is typically carried out by modeling the optical impulse response of the imaging system and fitting model functions to the data. However, such models are only well-suited to isolated molecules, reducing the number of molecules in the field of view and limiting temporal resolution in super resolution microscopy. This issue has incited a series of efforts to increase the density of fluorescent molecules imaged in a single frame while developing appropriate models for dense localization.

In fluorescence microscopy, each pixel is treated as a Poisson random variable (Smith 2010; Nehme 2020; Chao 2016), with expected value

$$\omega = i_0 \int O(u)du \int O(v)dv \quad (10)$$

where  $i_0 = \eta N_0 \Delta$ . The scalar parameters  $\eta, \Delta$  are the photon detection probability of the sensor and the exposure time, respectively. Without loss of generality, we assume  $\eta = \Delta = 1$ . Most importantly,  $N_0$  represents the signal amplitude, which we assume maintains a fixed value. The optical impulse response  $O(u, v)$  is often approximated as a 2D isotropic Gaussian with standard deviation  $\sigma$  (Zhang 2007). This approximation has the convenient property, that the effects of pixelation can be expressed in terms of error functions. For example, given a fluorescent emitter located at  $\theta = (u_0, v_0)$ , we have that

$$\int O(u)du = \frac{1}{2} \left( \operatorname{erf} \left( \frac{u_k + \frac{1}{2} - u_0}{\sqrt{2}\sigma} \right) - \operatorname{erf} \left( \frac{u_k - \frac{1}{2} - u_0}{\sqrt{2}\sigma} \right) \right) \quad (11)$$

where we have used the common definition  $\operatorname{erf}(z) = \frac{2}{\sqrt{\pi}} \int_0^z e^{-t^2} dt$ . Our generative model also incorporates a normally distributed white noise per pixel  $\zeta$  with offset  $o$  and variance  $\sigma^2$ . Ultimately, we have a Poisson component of the signal, which scales with  $N_0$  and a Gaussian component, which does not.

Consider,

$$\zeta_k - o_k + \sigma_k^2 \sim \mathcal{N}(\sigma_k^2, \sigma_k^2) \approx \text{Poisson}(\sigma_k^2) \quad (12)$$

Since  $\mathbf{x}_k = \mathbf{s}_k + \zeta_k$ , we transform  $\mathbf{x}'_k = \mathbf{x}_k - o_k + \sigma_k^2$ , which is distributed according to